

Data-driven identification of a 2D wave equation model with port-Hamiltonian structure

Charles Poussot-Vassal^{1,†}, Denis Matignon², Ghislain Haine² and Pierre Vuillemin¹ [✉]

November 30, 2022

Abstract

We consider a two-dimensional wave equation, for which the discretized version preserves the passive port-Hamiltonian form. In this work, we detail a procedure to construct a reduced order model of this use-case, on the basis of frequency-domain data, that preserves the passivity property and the port-Hamiltonian structure. The proposed scheme is based on Benner et al. contribution [1], which has been adapted to handle non-strictly passive model, and to handle numerical issues observed when applying the Loewner framework on such a complex configuration.

1 Introduction

1.1 Foreword

We are interested in an efficient numerical representation of the wave equation on a 2D domain Ω , with actuators and sensors that are *collocated* at the boundary $\partial\Omega$; the PDE model is first described as a distributed port-Hamiltonian system (pHs) (see the pioneering work [2], and [3] for a recent overview), second discretized in a structure-preserving manner thanks to the Partitioned Finite Element Method (PFEM) [4]. If in 1D with physical parameters ρ , T which are uniform in space $(0, \ell)$, the input-output transfer function is easy to compute ($\mathbf{H}(s) = Z_c \tanh(s\ell/c)$ with $Z_c = \sqrt{\rho T}$ and $c = \sqrt{T/\rho}$), the task becomes more difficult with varying parameters; in 2D it becomes almost impossible with a general geometric domain, heterogeneous and anisotropic parameters. However, a high-fidelity numerical model, or Full Order Model (FOM),

^{**}This work has been supported by the AID (Agence de l'Innovation de Défense) from the French Ministry of the Armed Forces (Ministère des Armées).

[†]Charles and Pierre are with ONERA – The French Aerospace Lab, 2 avenue Edouard Belin, Toulouse 31400, France.

[‡]Denis and Ghislain are with ISAE-SUPAERO, Université de Toulouse, 10, avenue Edouard Belin, Toulouse 31400, France.

[✉] Corresponding author: charles.poussot-vassal@onera.fr

taking all these important properties into account can be computed at the discrete level, see [5].

This model results in a highly complex linear port-Hamiltonian system, embedding a very large number of internal state variables, a quite large number of inputs and outputs, and thus large-scale matrices. Such a high dimension is a limiting factor for simulation, optimisation, analysis and control. Indeed, ODE and DAE solvers may run into numerical issues and catastrophic errors propagation, and the computational burden limit the many query simulation-based optimisation steps. Computing simplified, easy to use dynamical models is one purpose of the model approximation and reduction discipline, which refers to a class of methodologies used for reducing the computational complexity of large-scale models (or data) of dynamical systems. The goal generally is to approximate the original system with a smaller and simpler system with the *same structure* and similar response characteristics as the original, the low-complexity model, also called a Reduced Order Model (ROM).

The Loewner Framework (LF) employed in this work is a *data-driven* model identification and reduction technique that was originally introduced in [6]. Using only measured data, the LF constructs surrogate models directly and with low computational effort. Its extension to pH model is proposed in [1]. For an overview of model reduction methods, we refer the reader to [7, 8] and to the references therein. Recently [9] gave an overview of physics-based reduction methods, and [10] presents a successful attempts to apply data-driven techniques to identification of pHs, at least on a 1D example.

1.2 Notations and preliminaries

The set of real and complex numbers of dimension n are denoted, respectively by \mathbb{R}^n and \mathbb{C}^n . The complex variable $\iota = \sqrt{-1}$. The notation $\mathbb{X}_\Lambda^n : \{x \in \mathbb{X}^n \setminus \Lambda\}$, where Λ denotes a finite number set (typically singularities) in \mathbb{X}^n ($\mathbb{X}^n = \{\mathbb{R}^n, \mathbb{C}^n\}$). The set of stable rational functions with bounded ∞ -norm along $\iota\mathbb{R}$, is denoted \mathcal{RH}_∞ . Similarly, \mathcal{RL}_∞ denotes the same set but for both stable and unstable functions. The identity matrix and the null matrix of dimension p read, respectively, I_p and 0_p . The Laplace variable is represented by $s \in \mathbb{C}$.

In this note we consider the following multi-input multi-output (MIMO) linear time invariant (LTI) continuous-time dynamical systems forms:

$$\begin{cases} E\dot{x}(t) &= Ax(t) + Bu(t), x(0) = 0 \\ y(t) &= Cx(t) \end{cases} \quad (1a)$$

$$\begin{cases} \dot{x}(t) &= Ax(t) + Bu(t), x(0) = 0 \\ y(t) &= Cx(t) + Dx(t) \end{cases} \quad (1b)$$

$$\begin{cases} M\dot{x}(t) &= (J-R)Qx(t) + (G-P)u(t), x(0) = 0 \\ y(t) &= (G+P)^\top Qx(t) + (N+S)u(t) \end{cases} \quad (1c)$$

where $x(t) \in \mathbb{R}^n$ and $u(t), y(t) \in \mathbb{R}^m$ are vector-valued functions denoting the internal variables, input and output of the system. In the standard descriptor (1a) and non-descriptor (1b) forms, we consider constant matrices $E, A \in \mathbb{R}^{n \times n}$, $B, C^\top \in \mathbb{R}^{n \times m}$

and $D \in \mathbb{R}^{m \times m}$. When considering the port-Hamiltonian form (1c), $M, J, R, Q \in \mathbb{R}^{n \times n}$, $G, P \in \mathbb{R}^{n \times m}$ and $N, S \in \mathbb{R}^{m \times m}$. For brevity, (1a) and (1b) are denoted $\Sigma := (E, A, B, C, 0_m)$ and $\Sigma := (I_n, A, B, C, D)$ respectively. Similarly, the port-Hamiltonian (pH) form (1c) is shortly denoted $\Sigma_{\text{pH}} := (M, Q, J, R, G, P, N, S)$. By introducing the co-energy variable $e(t) = Qx(t)$, (1c) boils down into $M\dot{x}(t) = (J - R)e(t) + (G - P)u(t)$ and $y(t) = (G + P)^\top e(t) + (N + S)u(t)$. The latter is the so-called *co-energy pH form* and is of specific meaning in the computation of the Hamiltonian, although not "natural" in dynamical systems. In each cases, we define the associated transfer functions as $\mathbf{H} : \mathbb{C}_\Lambda \mapsto \mathbb{C}^{m \times m}$, where $\mathbf{H}(s) = C(sE - A)^{-1}B$ for (1a), $\mathbf{H}(s) = C(sI - A)^{-1}B + D$ for (1b) and $\mathbf{H}(s) = (G + P)^\top Q(sM - (J - R)Q)^{-1}(G - P) + (N + S)$ for (1c)¹. On the basis of \mathbf{H} , let us denote the spectral density as

$$\Phi_{\mathbf{H}}(s) := \mathbf{H}(s) + \mathbf{H}^\top(-s). \quad (2)$$

In addition, let us remind the following definitions, necessary to characterise a pH system.

Definition 1 (Positive realness) *For all $\omega \in \mathbb{R}$, the rational transfer $\mathbf{H}(s)$ is called strictly positive-real if $\Phi_{\mathbf{H}}(i\omega) \succ 0$ and positive-real if $\Phi_{\mathbf{H}}(i\omega) \succeq 0$.*

Definition 2 (Stability) *The rational transfer function $\mathbf{H}(s)$ is called asymptotically stable if its singularities Λ are in the open left-half plane, and called stable if its singularities Λ are in the closed left-half plane with any pole occurring on $i\mathbb{R}$ being not repeated.*

Definition 3 (Passivity) *The rational transfer function $\mathbf{H}(s)$ is called strictly passive if it is strictly positive real and asymptotically stable, and stable if positive real and stable.*

1.3 Contribution statement

This note is mainly an application of the LF initially proposed by [6] to identify ROM of the form (1a)-(1b), and which has been extended by [1] to identify port-Hamiltonian ROM (pH-ROM) as defined in (1c). The contributions of this paper, being methodological and application-oriented one, are the following:

- First to propose a methodological adjustment of [1], in order to identify pH models where the original system is passive but not strictly.
- Second, to add in [1]'s algorithm an intermediate stability enforcement step. This latter facilitate the numerical computation of spectral zeros, and more specifically, preserves the number of right hand side zeros. This step is performed using [11]'s approach.
- Third, to apply the proposed process to a highly dimensional ($n \gg 10^4$) and highly MIMO ($m \gg 1$) system, embedding a rich dynamic: the wave equation.

¹Here Λ denotes the singularities being the eigenvalues of (A, E) pencil in (1a), of A in (1b) and of $((J - R)Q, M)$ in (1c).

1.4 Paper organisation

The paper is organised as follows: §2 presents the considered 2D wave equation, being an infinite-dimensional model discretized in a structure-preserving manner, with guaranteed stability and passivity, thus leading to a high-order finite-dimensional port-Hamiltonian system of the form (1c). Then, in §3 we construct a pH-ROM approximation of the latter, using an adaptation of the data-driven LF of [1]. Illustrations and numerical results are given in §4. Conclusions and perspectives are drawn in §5.

2 The 2D wave equation

2.1 Port-Hamiltonian formulation

Let us consider the vertical deflection from equilibrium w of a 2D membrane $\Omega \subset \mathbb{R}^2$. Denoting ρ the mass density and T the Young's modulus of the membrane, a positive-definite symmetric tensor, leads to the damped wave equation, recast as a pHs: in [12]

$$\rho(x) \frac{\partial^2}{\partial t^2} w(t, x) + \varepsilon(x) \frac{\partial}{\partial t} w(t, x) - \operatorname{div} (T(x) \cdot \mathbf{grad} (w(t, x))) = 0, \quad t \geq 0, x \in \Omega,$$

where ε is a positive damping parameter, together with Neumann boundary control

$$(T(x) \cdot \mathbf{grad} (w(t, x))) \cdot \mathbf{n} = u_\partial(t, x), \quad t \geq 0, x \in \partial\Omega,$$

where \mathbf{n} is the outward normal to Ω . The Hamiltonian is the total mechanical energy, given as the sum of potential and kinetic energies

$$\begin{aligned} \mathcal{H}(t) := & \frac{1}{2} \int_{\Omega} (\mathbf{grad} (w(t, x)))^\top \cdot T(x) \cdot \mathbf{grad} (w(t, x)) \, dx \\ & + \frac{1}{2} \int_{\Omega} \rho(x) \left(\frac{\partial}{\partial t} w(t, x) \right)^2 \, dx, \quad t \geq 0. \end{aligned} \quad (3)$$

Taking the strain and the linear momentum

$$\alpha_q := \mathbf{grad} (w), \quad \alpha_p := \frac{\partial}{\partial t} w,$$

as energy variables, the Hamiltonian rewrites

$$\begin{aligned} \mathcal{H}(t) = & \mathcal{H}(\alpha_q(t, \cdot), \alpha_p(t, \cdot)) \\ = & \frac{1}{2} \int_{\Omega} (\alpha_q(t, x))^\top \cdot T(x) \cdot \alpha_q(t, x) \, dx + \frac{1}{2} \int_{\Omega} \frac{\alpha_p^2(t, x)}{\rho(x)} \, dx. \end{aligned} \quad (4)$$

The co-energy variables are by definition the variational derivatives of the Hamiltonian

$$e_q := \delta_{\alpha_q} \mathcal{H} = T \cdot \alpha_q, \quad e_p := \delta_{\alpha_p} \mathcal{H} = \frac{\alpha_p}{\rho},$$

i.e. the stress and the velocity respectively. These equalities are the constitutive relations which close the dynamical system.

Thanks to these variables, the wave equation writes as a port-Hamiltonian system

$$\begin{pmatrix} \frac{\partial}{\partial t} \alpha_q \\ \frac{\partial}{\partial t} \alpha_p \end{pmatrix} = \begin{bmatrix} 0 & \mathbf{grad} \\ \text{div} & -\varepsilon \end{bmatrix} \begin{pmatrix} e_q \\ e_p \end{pmatrix}, \quad \begin{cases} e_q = T \cdot \alpha_q, \\ e_p = \frac{\alpha_p}{\rho}, \end{cases}$$

$$\begin{cases} u_\partial = e_q \cdot \mathbf{n}, \\ y_\partial = e_p |_{\partial\Omega} \end{cases}.$$

The power balance satisfied by the Hamiltonian is

$$\frac{d}{dt} \mathcal{H} = \langle u_\partial, y_\partial \rangle_{\partial\Omega} - \int_\Omega \varepsilon |e_p|^2 \leq \langle u_\partial, y_\partial \rangle_{\partial\Omega}, \quad (5)$$

proving passivity. To get rid of the algebraic constraints induced by the constitutive relations, one rewrites the port-Hamiltonian system as

$$\begin{bmatrix} T^{-1} & 0 \\ 0 & \rho \end{bmatrix} \begin{pmatrix} \frac{\partial}{\partial t} e_q \\ \frac{\partial}{\partial t} e_p \end{pmatrix} = \begin{bmatrix} 0 & \mathbf{grad} \\ \text{div} & -\varepsilon \end{bmatrix} \begin{pmatrix} e_q \\ e_p \end{pmatrix}, \quad \begin{cases} u_\partial = e_q \cdot \mathbf{n}, \\ y_\partial = e_p |_{\partial\Omega}, \end{cases}$$

also known as the *co-energy formulation*. This allows to get a simple Ordinary Differential Equation (ODE) at the discrete level (instead of a Differential Algebraic Equation (DAE) in general).

2.2 Structure-preserving discretization

Let ϕ_q , φ_p and ψ be vector-valued, scalar-valued and boundary scalar-valued test functions respectively. The weak formulation reads

$$\begin{cases} \int_\Omega \phi_q \cdot T^{-1} \cdot \frac{\partial}{\partial t} e_q = \int_\Omega \phi_q \cdot \mathbf{grad}(e_p), \\ \int_\Omega \varphi_p \rho \frac{\partial}{\partial t} e_p = \int_\Omega \varphi_p \text{div}(e_q) - \int_\Omega \varphi_p \varepsilon e_p, \\ \int_{\partial\Omega} \psi y_\partial = \int_{\partial\Omega} \psi e_p. \end{cases}$$

The integration by parts of the second line makes $u_\partial = e_q \cdot \mathbf{n}$ appear

$$\begin{cases} \int_\Omega \phi_q \cdot T^{-1} \cdot \frac{\partial}{\partial t} e_q = \int_\Omega \phi_q \cdot \mathbf{grad}(e_p), \\ \int_\Omega \varphi_p \rho \frac{\partial}{\partial t} e_p = - \int_\Omega \mathbf{grad}(\varphi_p) \cdot e_q + \int_{\partial\Omega} \varphi_p u_\partial \\ \quad \quad \quad - \int_\Omega \varphi_p \varepsilon e_p, \\ \int_{\partial\Omega} \psi y_\partial = \int_{\partial\Omega} \psi e_p. \end{cases}$$

Let $(\phi_q^i)_{1 \leq i \leq N_q}$, $(\varphi_p^j)_{1 \leq j \leq N_p}$ and $(\psi^k)_{1 \leq k \leq N_\partial}$ be finite element families for q -type, p -type and boundary-type variables. Variables are approximated in their

respective finite element family

$$e_q^d(t, x) := \sum_{i=1}^{N_q} e_q^i(t) \phi_q^i(x), \quad e_p^d(t, x) := \sum_{j=1}^{N_p} e_p^j(t) \phi_p^j(x),$$

$$u_\partial^d(t, x) := \sum_{k=1}^{N_\partial} u_\partial^k(t) \psi^k(x), \quad y_\partial^d(t, x) := \sum_{k=1}^{N_\partial} y_\partial^k(t) \psi^k(x).$$

Denoting \underline{x} the (time-varying) vector of coordinates of the discretisation \star^d of \star in its respective finite element family, the discrete system reads

$$\underbrace{\begin{bmatrix} M_q & 0 & 0 \\ 0 & M_p & 0 \\ 0 & 0 & M_\partial \end{bmatrix}}_M \begin{pmatrix} \frac{d}{dt} e_q(t) \\ \frac{d}{dt} e_p(t) \\ -y_\partial(t) \end{pmatrix} = \underbrace{\begin{bmatrix} 0 & G & 0 \\ -G^\top & -M_\varepsilon & B \\ 0 & -B^\top & 0 \end{bmatrix}}_{J-R} \begin{pmatrix} e_q(t) \\ e_p(t) \\ u_\partial(t) \end{pmatrix}$$

where

$$(M_q)_{ij} := \int_\Omega \phi_q^i \cdot T^{-1} \cdot \phi_q^j, \quad (M_p)_{ij} := \int_\Omega \phi_p^i \rho \phi_p^j,$$

$$(M_\varepsilon)_{ij} := \int_\Omega \phi_p^i \varepsilon \phi_p^j, \quad (M_\partial)_{ij} := \int_{\partial\Omega} \psi^i \psi^j,$$

and

$$(G)_{ij} := \int_\Omega \phi_q^i \cdot \mathbf{grad}(\phi_p^j), \quad (B)_{jk} := \int_{\partial\Omega} \phi_p^j \psi^k.$$

By definition, the discrete Hamiltonian is equal to the continuous Hamiltonian evaluated in the approximated variables. As we are working with the co-energy formulation, a first step is to restate the Hamiltonian in terms of co-energy variables

$$\mathcal{H} = \frac{1}{2} \int_\Omega e_q \cdot T^{-1} \cdot e_q + \frac{1}{2} \int_\Omega \rho (e_p)^2.$$

Then, the discrete Hamiltonian is defined as

$$\mathcal{H}^d := \frac{1}{2} \int_\Omega e_q^d \cdot T^{-1} \cdot e_q^d + \frac{1}{2} \int_\Omega \rho (e_p^d)^2.$$

After straightforward computations, it comes

$$\mathcal{H}^d(t) = \frac{1}{2} \underline{e}_q(t)^\top M_q \underline{e}_q(t) + \frac{1}{2} \underline{e}_p(t)^\top M_p \underline{e}_p(t),$$

and the *discrete* power balance follows

$$\begin{aligned} \frac{d}{dt} \mathcal{H}^d(t) &= \underline{u}_\partial(t)^\top M_\partial \underline{y}_\partial(t) - \underline{e}_p(t)^\top M_\varepsilon \underline{e}_p(t) \\ &\leq \underline{u}_\partial(t)^\top M_\partial \underline{y}_\partial(t), \end{aligned}$$

mimicking (5) exactly at the discrete level. The pH full order model (pH-FOM) is thus given by the a realization Σ_{pH} in the form (1c). The convergence of the numerical

method is assessed in [13], where the optimal selection of families of Finite Elements is proved. The objective is to use these matrices and the associated transfer function \mathbf{H} to generate *data*, through the dedicated SCRIMP simulator², presented in [14]. These data shall serve the construction of a pH-ROM, as explained in §3.

3 Port-Hamiltonian identification in the Loewner framework

We are interested in identifying a MIMO ROM preserving the pH structure of Σ_{pH} , using a data-driven framework. To do so, we follow the approach of [1] which extends the LF originally presented in [6]. The latter is first reminded in §3.1, while the former is presented in §3.2. The methodological and practical numerical adjustments to [1]’s algorithm, to cope with non-strictly passive systems and numerical issues, are detailed in §3.3.

3.1 Preliminaries

The LF offers tools for the reduction, approximation and identification of dynamical systems based on frequency-domain data. Let us denote as the *right and left data* the following sets (where $j = 1, \dots, k$ and $i = 1, \dots, q$):

$$\{\lambda_j, \mathbf{r}_j, \mathbf{w}_j\} \text{ and } \{\mu_i, \mathbf{l}_i^\top, \mathbf{v}_i^\top\}, \quad (6)$$

where $\lambda_j \in \mathbb{C}$ and $\mu_i \in \mathbb{C}$ are the right and left interpolation points. Then, $\mathbf{r}_j \in \mathbb{C}^{m \times 1}$ and $\mathbf{l}_i^\top \in \mathbb{C}^{1 \times m}$ are the right and left tangential directions. Both points and directions lead to the right $\mathbf{H}(\lambda_j)\mathbf{r}_j = \mathbf{w}_j \in \mathbb{C}^{m \times 1}$ and left $\mathbf{l}_i^\top \mathbf{H}(\mu_i) = \mathbf{v}_i^\top \in \mathbb{C}^{1 \times m}$ tangential responses. In the considered case, $\mathbf{H}(s_k)$ is the evaluation of the high dimensional pH-FOM (§2) at point $s_k \in \mathbb{C}$. Based on (6), the LF seeks for $\hat{\Sigma} : (\hat{E}, \hat{A}, \hat{B}, \hat{C}, 0_m)$, whose transfer function $\hat{\mathbf{H}}(s)$ satisfies tangential interpolatory conditions $\hat{\mathbf{H}}(\lambda_j)\mathbf{r}_j = \mathbf{w}_j$ and $\mathbf{l}_i^\top \hat{\mathbf{H}}(\mu_i) = \mathbf{v}_i^\top$. By using the matrix formulation, the right data read

$$\begin{cases} \Lambda &= \mathbf{diag} [\lambda_1, \dots, \lambda_k] \in \mathbb{C}^{k \times k}, \\ \mathbf{R} &= \begin{bmatrix} \mathbf{r}_1 & \mathbf{r}_2 & \dots & \mathbf{r}_k \end{bmatrix} \in \mathbb{C}^{m \times k}, \\ \mathbf{W} &= \begin{bmatrix} \mathbf{w}_1 & \mathbf{w}_2 & \dots & \mathbf{w}_k \end{bmatrix} \in \mathbb{C}^{m \times k} \end{cases}, \quad (7)$$

and the left data read

$$\begin{cases} \mathbf{M} &= \mathbf{diag} [\mu_1, \dots, \mu_q] \in \mathbb{C}^{q \times q} \\ \mathbf{L}^\top &= \begin{bmatrix} \mathbf{l}_1 & \mathbf{l}_2 & \dots & \mathbf{l}_q \end{bmatrix} \in \mathbb{C}^{m \times q} \\ \mathbf{V}^\top &= \begin{bmatrix} \mathbf{v}_1 & \mathbf{v}_2 & \dots & \mathbf{v}_q \end{bmatrix} \in \mathbb{C}^{m \times q} \end{cases}. \quad (8)$$

Then, by defining the j, i -th entry of the Loewner and shifted Loewner matrix as

$$(\mathbb{L})_{ij} = \frac{\mathbf{v}_i^\top \mathbf{r}_j - \mathbf{l}_i^\top \mathbf{w}_j}{\mu_i - \lambda_j} \text{ and } (\mathbb{M})_{ij} = \frac{\mu_i \mathbf{v}_i^\top \mathbf{r}_j - \mathbf{l}_i^\top \mathbf{w}_j \lambda_j}{\mu_i - \lambda_j}, \quad (9)$$

²<https://g-haine.github.io/scrimp/>

the resulting system realization $\hat{\Sigma} := (\hat{E}, \hat{A}, \hat{B}, \hat{C}, 0_m) = (-\mathbb{L}, -\mathbb{M}, \mathbf{V}, \mathbf{W}, 0_m)$ which transfer function $\hat{\mathbf{H}}(s) = \mathbf{W}(\mathbb{M} - s\mathbb{L})^{-1}\mathbf{V}$ (tangentially) interpolates the *data*. In addition, it follows that Loewner matrices satisfy the Sylvester equations $\mathbf{M}\mathbb{L} - \mathbb{L}\Lambda = \mathbf{V}\mathbf{R} - \mathbf{L}\mathbf{W}$ and $\mathbf{M}\mathbb{M} - \mathbb{M}\Lambda = \mathbf{M}\mathbf{V}\mathbf{R} - \mathbf{L}\mathbf{W}\Lambda$. Importantly, if the data have been generated by a linear rational model, the rational order $r = \mathbf{rank}(s\mathbb{L} - \mathbb{M}) = \mathbf{rank}([\mathbb{L}, \mathbb{M}]) = \mathbf{rank}([\mathbb{L}^H, \mathbb{M}^H]^H)$ recovers the one of the minimal realisation of the generating system, as well as its McMillan degree ν , given by $\nu = \mathbf{rank}(\mathbb{L})$. In conclusion, the LF allows approximating and identifying frequency-domain responses, while also encoding fundamental realisation-oriented properties, *e.g.* the McMillan degree and the minimal realisation order. These features make this approach central in the realisation theory. Refer to Gosea et al. in [8] for a recent overview.

3.2 Dealing with strict passivity

3.2.1 General ideal and assumptions

Applying the LF to *data* generated by a passive system \mathbf{H} do not necessarily lead to a passive transfer $\hat{\mathbf{H}}$ or realisation $\hat{\Sigma}$. This issue is solved in Benner et al. [1] by mean of an specific *right and left data* selection. This result is briefly recalled here after reminding the following main (limiting) statements, assumed to be true in [1].

Assumption 1 (Strictly passive) *First, in [1], authors assume that the system, which generates the data, is strictly passive, implying that the transfer matrix \mathbf{H} is proper and singularities cannot be on the imaginary axis or at infinity. Therefore, $D^\top + D \succ 0$.*

Assumption 2 (Stability) *In [1], the resulting $\hat{\Sigma}$ model, obtained after a first identification in the standard LF, leads to a pencil $(\mathbb{M}, \mathbb{L}) = (\hat{A}, \hat{E})$, being assumed to be stable, i.e. $\Lambda \in \mathbb{C}_-$.*

3.2.2 Procedure as given in [1]

First, let $\hat{\mathbf{H}}$ be identified by the LF, on the basis of a real and strictly passive transfer function \mathbf{H} , where the D -term is removed to avoid rank deflecting $\hat{E} = \mathbb{L}$ matrix. It results in $\hat{\mathbf{H}}$ where McMillan degree ν is equal to the (minimal) realisation order r , since no polynomial term appear (because of the strict passivity and D -term removal). Note that r may be automatically selected by the rank revealing factorisation of the LF or be chosen smaller if ROM is sought. This identified model $\hat{\mathbf{H}}$ with realisation $\hat{\Sigma}$ is now used to estimate the associated spectral zeros and directions pairs, denoted (ξ_j, \mathbf{x}_j) such that

$$\Phi_{\hat{\mathbf{H}}}(\xi_j)\mathbf{x}_j = 0. \quad (10)$$

This pair can be computed by solving the following low order generalized eigenvalue problem (see [15, 1]):

$$\begin{bmatrix} 0 & \hat{A} & \hat{B} \\ \hat{A}^\top & 0 & \hat{C}^\top \\ \hat{B}^\top & \hat{C} & D + D^\top \end{bmatrix} \begin{bmatrix} p_j \\ q_j \\ \mathbf{x}_j \end{bmatrix} = \xi_j \begin{bmatrix} 0 & \hat{E} & 0 \\ \hat{E}^\top & 0 & 0 \\ 0 & 0 & 0 \end{bmatrix} \begin{bmatrix} p_j \\ q_j \\ \mathbf{x}_j \end{bmatrix}. \quad (11)$$

Note that this latter requires a realisation and is thus computed after a first identification step done *e.g.* in the LF. According to Assumptions 1 and 2, this eigen-problem has r zeros in the open right half-plane, r zeros in the open left half-plane and has no zeros on the imaginary axis. By selecting the *right and left strictly passive data* as $(i, j = 1, \dots, r = k = q, \lambda_j \leftarrow \xi_j$ and $\mathbf{r}_j \leftarrow \mathbf{x}_i$),

$$\{\lambda_j, \mathbf{r}_j, \mathbf{w}_j\} \text{ and } \{-\bar{\lambda}_i, \mathbf{r}_i^H, -\mathbf{v}_i^H\}, \quad (12)$$

one gets, $\mathbf{M} = -\Lambda^H$, $\mathbf{L} = \mathbf{R}$ and $\mathbf{V} = -\mathbf{W}^H$. Therefore, by construction (9), one obtains an Hermitian $\mathbb{L} \in \mathbb{C}^{r \times r}$ and a skew symmetric $\mathbb{M} \in \mathbb{C}^{r \times r}$ matrix. By setting, $\mathbf{H}(\infty) = D$ (which may be estimated by sampling in very high frequency), one recovers an $m \times m$ real transfer function $\hat{\mathbf{H}}$ (real matrices are straightforwardly obtained if data are sampled with complex conjugate frequencies and by applying a unitary projection as detailed in [16, 8]). As $\mathbb{L} \succ 0$, one may apply the Cholesky decomposition $\mathbb{L} = T^\top T$. Then the *normalized pH model* is obtained as $\Sigma_{\text{n-pH}} := (I_n, T\hat{A}T^{-1}, T\hat{B}, \hat{C}T^{-1}, D)$, with form (1b). By defining

$$\mathbf{S} := \begin{bmatrix} -T\hat{A}T^{-1} & -T\hat{B} \\ \hat{C}T^{-1} & D \end{bmatrix}, \quad (13)$$

one obtains the equivalent pH-form (1c) by solving

$$\begin{bmatrix} -J & -G \\ G^\top & N \end{bmatrix} := \frac{\mathbf{S} - \mathbf{S}^\top}{2} \text{ and } \begin{bmatrix} R & P \\ P^\top & S \end{bmatrix} := \frac{\mathbf{S} + \mathbf{S}^\top}{2}. \quad (14)$$

However, this approach suffers from two limitations. The first one stands in the assumption that the original model generating the data should be *strictly* passive, and thus is cannot be applied to the *non-strictly* passive model presented in §2. The second one is more numerical: in practice Loewner pencil (\mathbb{M}, \mathbb{L}) of stable functions \mathbf{H} may not be necessarily stable (see [17]). Next, we propose two steps to overcome these limitations, while preserving the pH-ROM structure.

3.3 Dealing with non-strict passivity and stability

3.3.1 Proposed modified algorithm

With reference to Algorithm 1 of [1], we suggest the following additional steps:

- Prior "Step 1", we suggest shifting the data with a positive scalar to translate the Nyquist response on the right hand side. Thus, the first step consists in applying a $D \leftarrow D + D_s$ if the model is available, or directly from the data, $\mathbf{w}_j \leftarrow \mathbf{w}_j + D_s$ and $\mathbf{v}_i \leftarrow \mathbf{v}_i + D_s$. This result in a data that are now strictly passive.
- After "Step 1", as Loewner does not ensures stability, we suggest a projection of the rational ROM $\hat{\mathbf{H}}$ with realisation $\hat{\Sigma}$ onto the \mathcal{RH}_∞ space, following [11]. This leads to a stable $\hat{\mathbf{H}} \leftarrow P_\infty(\hat{\mathbf{H}})$.
- After "Step 6", based on the normalised (strictly proper) realisation $\hat{\Sigma}_{\text{n-pH}}$, recover the original non-strictly passive model, by simply applying $S \leftarrow S - D_s$ after solving (14), leading to the pH-ROM fitting the original data.

3.3.2 Comments

#1 and #3's bullets Should the original model, and therefore associated data, be non strictly passive, but only passive. This typically occurs when no direct feed-through term exist. As a consequence, the resulting spectral zeros exhibit zeros on the imaginary axis. The first and last bullets address this points. One simply shifts the original problem to apply the strict-passive approach of [1].

#2's bullet The rational model obtained through the Loewner framework and denoted $\hat{\mathbf{H}}$ may present some so-called unstable singularities. Therefore we suggest a *post stabilisation* using the procedure presented in [11]. This latter consists in projecting the rational model $\hat{\mathbf{H}} \in \mathcal{R}\mathcal{L}_\infty$ onto its closest stable subset $\mathcal{R}\mathcal{L}_\infty$, here using the \mathcal{H}_∞ -norm, leading to a stable model of the same dimension r . Mathematically, and as exposed in details in [11], given a rational model $\hat{\mathbf{H}} \in \mathcal{R}\mathcal{L}_\infty$ equipped with realisation $\hat{\Sigma}$, one aims at finding $P_\infty(\hat{\mathbf{H}}) \in \mathcal{R}\mathcal{H}_\infty$ such that,

$$P_\infty(\hat{\mathbf{H}}) = \arg \inf_{\mathbf{G} \in \mathcal{R}\mathcal{H}_\infty} \|\hat{\mathbf{H}} - \mathbf{G}\|_{\mathcal{H}_\infty}. \quad (15)$$

The proof and procedure to obtain $P_\infty(\hat{\mathbf{H}})$ are detailed in [11]. The key steps consists in performing the stable and unstable part separation, then solving two Lyapunov equations (of reduced order). Applying this post-treatment to the Loewner-based approximate thus preserves the number of singularities and, hopefully, the accuracy and interpolatory properties.

4 Numerical use-case

The considered model \mathbf{H} is a 2D wave equation, which support Ω is L-shaped. The resulting discretised pH model is equipped with a realisation Σ_{pH} in pH-form as in (1c). It has the following characteristics: $n = 63,409$ and $m = 604$. For illustration, we will now consider to sub-cases. First, (i) the SISO case: $m = 1$, where we consider the first input / output pair only and second, (ii) the MIMO case: $m = 3$, where we consider the following input / output index pairs $\{1, 2, 496\}$ only. One may notice that the model is stable, poorly damped, but not strictly passive, thus spectral zeros on $i\mathbb{R}$ should unlikely occur, resulting in an non verified Assumption 1. In what follows, we denote as:

- *Data*, the original system presented in §2 sampled along $i\omega_l$, where ω_l are $l = 1, \dots, 300$ logarithmically spaced values between 10^{-1} and $10^{3.5}$ rad/s.
- *Loewner*, the dynamical model obtained with the standard LF, in the form (1a).
- *pH-Loewner*, the dynamical model obtained with the proposed adjustment of [1], in the form (1c).

In each case, we also use the denomination *shifted* to point the data or model shifted and with *post-stability enforcement*, to ensure strict dissipativity.

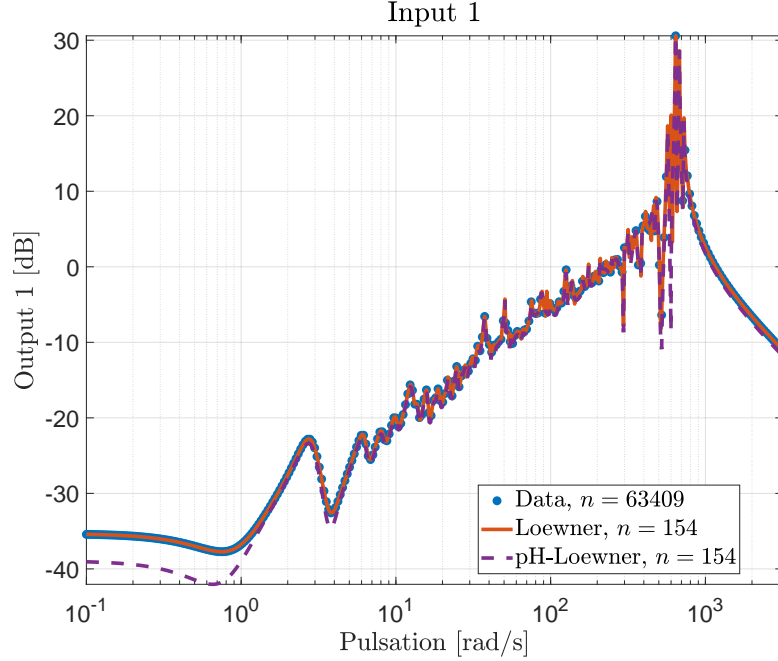


Figure 1: Frequency response of the original data, the Loewner and the pH-Loewner models.

4.1 SISO case: process illustration

First, Figure 1 presents the frequency response of the original *data*, compared to the (non-dissipative and non-stable) *Loewner* model and the *pH-Loewner* one, illustrating the nice restitution of the frequency response in both cases. Here, the *pH-Loewner* is passive and embeds the expected pH-structure.

Figure 2 (3) show the (zoomed) spectral zeros. The *Loewner* model has many zeros along or close to the imaginary axis (\times). Indeed, between the real band $[-1, 1] \times 10^{-10}$, we count 4 zeros and between $[-1, 1] \times 10^{-9}$, 12. This is an issue for selecting the positive interpolation points. This problem is solved by the proposed algorithm modification, thanks to both *post-stability enforcement* and *data-shift*. Indeed, the *pH-Loewner (shifted)* shows zeros far from this limit ($+$). Then, after applying the shift-back, one recovers the sought *pH-Loewner* model (\bullet), where spectral zeros are back on the imaginary axis. Note that without the proposed algorithm adjustments, no solution can be found as the \mathbb{L} matrix is not positive definite and Cholesky decomposition proves impossible.

As a complement, the same Bode magnitude diagram is show on Figure 4, where the pH-model is now reduced to an order 30, while in the previous illustration, automatic order selection was performed by the rank revealing decomposition of the LF.

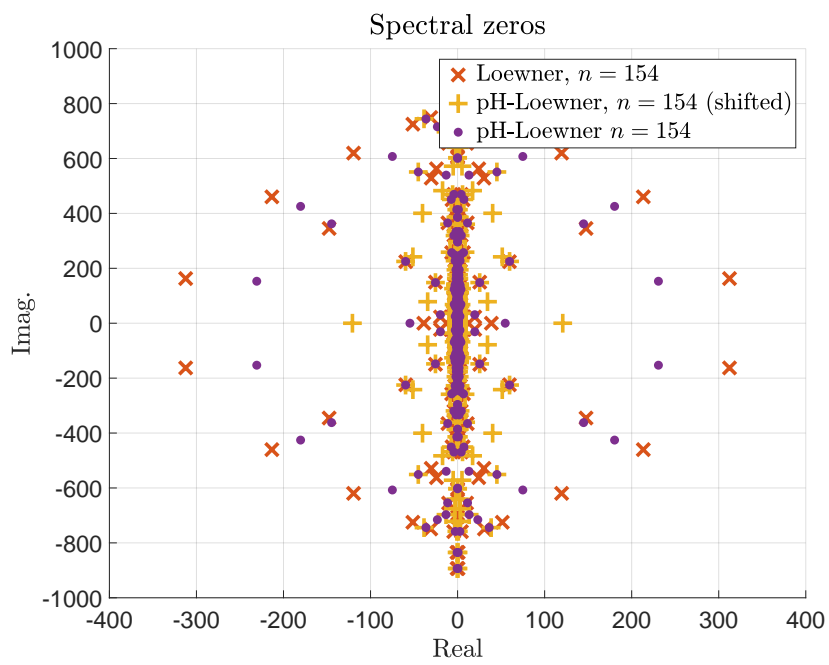


Figure 2: Spectral zeros response of the Loewner, the Loewner (applied on the shifted data) and the pH-Loewner models.

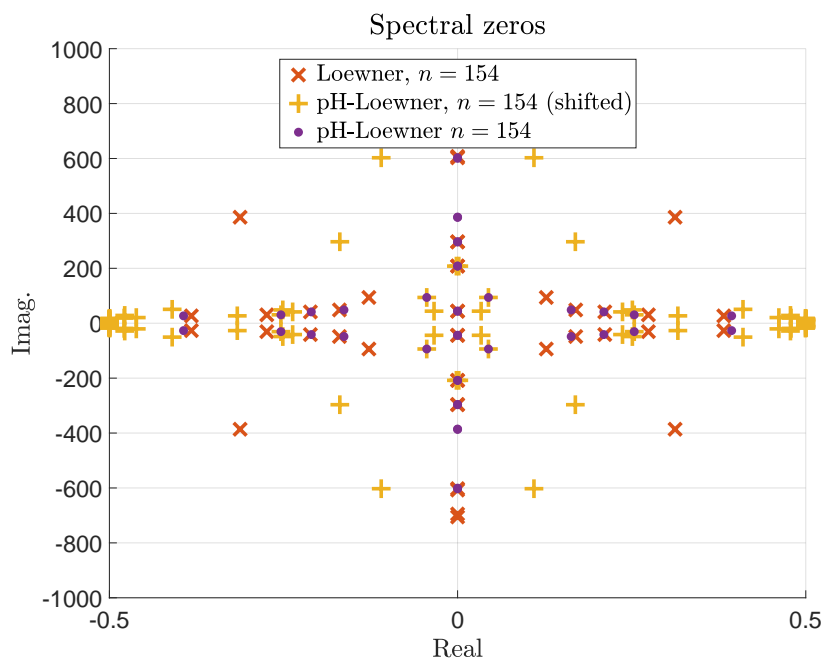


Figure 3: Spectral zeros response of the Loewner, the Loewner (applied on the shifted data) and the pH-Loewner models.

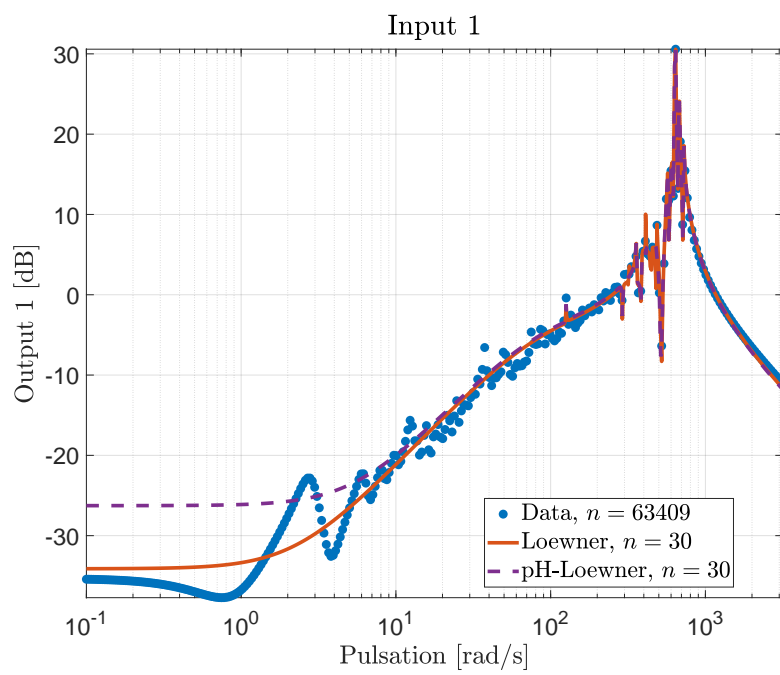


Figure 4: Frequency response of the original data, the Loewner and the pH-Loewner models (with order reduction).

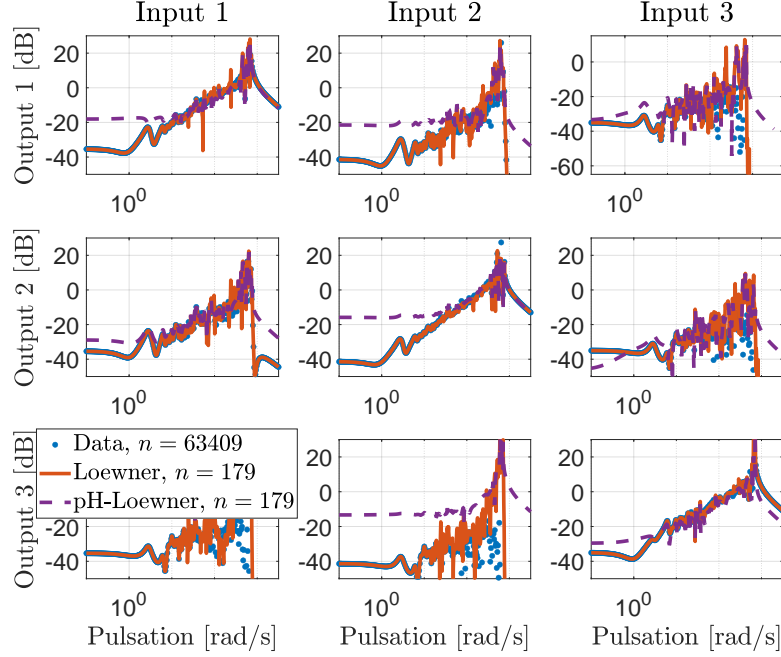


Figure 5: Frequency response of the original data, the Loewner and the pH-Loewner models.

4.2 MIMO case

As mentioned, one important challenge in this application in addition to the complexity of the dynamics of the wave equation, is its large number of inputs and outputs ($m = 604$). So far, applying the above process to this large MIMO system led to non fully satisfactory results. However, up to $m = 10$, good approximation have been observed. In Figure 5, we illustrate the frequency magnitude response for $m = 3$, where the first two inputs / outputs are spatially close, whereas the third one is far from the others.

From Figure 5, we appreciate the fact that diagonal elements (more energetic since the model is collocated) are well reproduced. Regarding the anti-diagonal ones, a good restitution is observed on channels (1,2) and (2,1) but not on (1,3), (2,3), (3,1) and (3,2). Indeed, these transfer are very different and less energetic than the other and thus not well approximated. This is due to the distance of the third input-output with respect to the first two. Future research will focus on this aspect, *e.g.* with a specific treatment of the tangential directions in (6).

5 Conclusions & perspectives

We have shown promising numerical results of a *data-driven* reduction technique applied to a 2D wave PDE, modelled as a pHs: it is obtained using the LF, and more specifically a modification of [1] using the frequency-responses generated by the matrices provided by the structure-preserving PFEM. The main modifications to [1] are (i) the data-shift to handle non-strictly passive models and (ii) the post-stability enforcement, to cope with numerical issues often encountered when applying the LF. These two steps were essential to achieve the presented results. Indeed, what is successful is the number of states that can be drastically reduced (from $n = 63,409$ to $n = 179$). However, the collocated input-output pairs have been tried on a SISO case, or on a MIMO case of small dimension ($m = 3, \dots, 10$), whereas to obtain a good approximation of the PFEM, the boundary should be discretized by, say, $m = 50, 100$ or more DoFs. Future development would consider handling a larger number of inputs-outputs. Moreover, another real world application in 2D is the heat equation with collocated normal heat flux control and temperature observation, resulting in a pH-DAE system, see [18]. Finally we have in view is the Maxwell's equations, see [19], where both the unknowns are 3D-vector fields, thus requiring even more the development of dedicated reduction methods. Other benchmarked pHs will be of interest also³.

References

- [1] P. Benner, P. Goyal, and P. V. Dooren, "Identification of port-hamiltonian systems from frequency response data," *Systems & Control Letters*, vol. 143, p. 104741, September 2020.
- [2] A. van der Schaft and B. Maschke, "Hamiltonian formulation of distributed-parameter systems with boundary energy flow," *Journal of Geometry and Physics*, vol. 42, no. 1-2, pp. 166–194, 2002.
- [3] R. Rashad, F. Califano, A. van der Schaft, and S. Stramigioli, "Twenty years of distributed port-Hamiltonian systems: a literature review," *IMA Journal of Mathematical Control and Information*, vol. 37, no. 4, pp. 1400–1422, 2020.
- [4] F. L. Cardoso-Ribeiro, D. Matignon, and L. Lefèvre, "A partitioned finite-element method for power-preserving discretization of open systems of conservation laws," *IMA J. Mathematical Control and Information*, vol. 38, no. 2, pp. 493–533, 2021.
- [5] A. Serhani, D. Matignon, and G. Haine, "A partitioned finite element method for the structure-preserving discretization of damped infinite-dimensional port-Hamiltonian systems with boundary control," in *Geometric Science of Information* (F. Nielsen and F. Barbaresco, eds.), vol. 11712 of *Lecture Notes in Computer Science*, pp. 549–558, Springer, 2019.

³<https://algopaul.github.io/PortHamiltonianBenchmarkSystems/>

- [6] A. Mayo and A. Antoulas, “A framework for the solution of the generalized realization problem,” *Linear Algebra and its Applications*, vol. 425, no. 2, pp. 634–662, 2007. Special Issue in honor of Paul Fuhrmann.
- [7] A. Antoulas, C. Beattie, and S. Gugercin, *Interpolatory methods for model reduction*. Philadelphia: SIAM Computational Science and Engineering, 2020.
- [8] I. Gosea, C. Poussot-Vassal, and A. Antoulas, “Data-driven modeling and control of large-scale dynamical systems in the Loewner framework,” *Handbook of Numerical Analysis*, vol. 23, no. Numerical Control: Part A, pp. 499–530, 2022.
- [9] O. Ghattas and K. Willcox, “Learning physics-based models from data: perspectives from inverse problems and model reduction,” *Acta Numerica*, pp. 445–554, 2021.
- [10] K. Cherifi and A. Brugnoli, “Application of data-driven realizations to port-Hamiltonian flexible structures,” in *IFAC-PapersOnLine*, vol. 54, (Berlin, Germany), pp. 180–185, Nov. 7th IFAC Workshop on Lagrangian and Hamiltonian Methods for Nonlinear Control (LHMNLC).
- [11] M. Kohler, “On the closest stable descriptor system in the respective spaces \mathcal{RH}_2 and \mathcal{RH}_∞ ,” *Linear Algebra and its Applications*, vol. 443, pp. 34–49, 2014.
- [12] M. Kurula and H. Zwart, “Linear wave systems on n-D spatial domains,” *International Journal of Control*, vol. 88, no. 5, pp. 1063–1077, 2015.
- [13] G. Haine, D. Matignon, and A. Serhani, “Numerical analysis of a structure-preserving space-discretization for an anisotropic and heterogeneous boundary controlled N -dimensional wave equation as a port-Hamiltonian system,” *Int. J. Numer. Anal. Mod.*, vol. 20, no. 1, pp. 92–133, 2023.
- [14] A. Brugnoli, G. Haine, A. Serhani, and X. Vasseur, “Numerical approximation of port-Hamiltonian systems for hyperbolic or parabolic PDEs with boundary control,” *Journal of Applied Mathematics and Physics*, vol. 9, pp. 1278–1321, June 2021. Supplementary material, <https://doi.org/10.5281/zenodo.3938600>.
- [15] J. Willems, “Dissipative dynamical systems part II: Linear systems with quadratic supply rates,” *Arch. Ration. Mech. Anal.*, vol. 45, pp. 352–393, 1972.
- [16] A. Antoulas, S. Lefteriu, and A. Ionita, *Model reduction and approximation theory and algorithms*, ch. A tutorial introduction to the Loewner framework for model reduction. SIAM, Philadelphia, P. Benner, A. Cohen, M. Ohlberger and K. Willcox Eds, 2016.
- [17] I. Gosea, C. Poussot-Vassal, and A. Antoulas, “On enforcing the stability of data-driven reduced-order models,” in *Proceedings of the IEEE Mediterranean Control Conference*, (Bari, Italy), June 2021.

- [18] A. Serhani, G. Haine, and D. Matignon, “Anisotropic heterogeneous n-D heat equation with boundary control and observation: II. structure-preserving discretization,” in *IFAC-PapersOnLine*, vol. 52, (Louvain-La-Neuve, Belgium), pp. 57–62, July 2019. 3rd IFAC Workshop on Thermodynamics Foundations of Mathematical Systems Theory (TFMST).
- [19] G. Haine, D. Matignon, and F. Monteghetti, “Structure-preserving discretization of Maxwell’s equations as a port-Hamiltonian system,” in *IFAC-PapersOnLine*, vol. 55, (Bayreuth, Germany), pp. 424–429, Sept. 2022. 25th IFAC Symposium on Mathematical Theory of Networks and Systems (MTNS).